Chemical Engineering Journal 219 (2013) 238–244

Contents lists available at SciVerse ScienceDirect

Chemical Engineering Journal

journal homepage: www.elsevier.com/locate/cej

Resorcinol modified hypercrosslinked poly(styrene-co-divinylbenzene) resin and its adsorption equilibriums, kinetics and dynamics towards *p*-hydroxylbenzaldehyde from aqueous solution

Jianhan Huang [a,b,*], Li Yang [a], Yunyi Zhang [a], Chunyue Pan [a,b], You-Nian Liu [a,b]

[a] College of Chemistry and Chemical Engineering, Central South University, Changsha 410083, China
[b] Key Laboratory of Resources Chemistry of Nonferrous Metals, Ministry of Education, Changsha 410083, China

HIGHLIGHTS

- Novel carbonyl and hydroxyl groups modified hypercrosslinked resins were synthesized.
- These resins possessed different adsorption selectivity.
- Surface energy heterogeneity of the resin could be described by Do's model.
- The dynamics matched the equilibrium and kinetics very well.
- The dynamic data could be described by Thomas model.

ARTICLE INFO

Article history:
Received 16 November 2012
Received in revised form 4 January 2013
Accepted 5 January 2013
Available online 11 January 2013

Keywords:
Hypercrosslinked poly (styrene-co-divinylbenzene) resin
Adsorption
p-Hydroxylbenzaldehyde
Equilibrium
Kinetics
Dynamics

ABSTRACT

A series of resorcinol modified hypercrosslinked poly(styrene-co-divinylbenzene) (PS) resins, named as HJ-H00, HJ-H02, HJ-H05, HJ-H10 and HJ-H15, were synthesized from macroporous cross-linked chloromethylated PS by adding 0%, 2%, 5%, 10% and 15% of resorcinol in the Friedel–Crafts reaction, and these resins were characterized and evaluated for adsorption of *p*-hydroxylbenzaldehyde from aqueous solution. The characterization indicated that these resins possessed different chemical structure and pore structure, indicative of their adsorption selectivity. HJ-H02 had the largest adsorption capacity towards *p*-hydroxylbenzaldehyde among the five resins and the mechanism was a combination of hydrogen bonding, micropore filling, capillary condensation and π–π stacking. Freundlich equation was suitable for fitting the equilibrium data and the isosteric adsorption enthalpies were applied to describe the surface energy heterogeneity of the resin. The pseudo-second-order rate equation-I was appropriate for the kinetic data and Thomas model was suitable for the dynamic data. The dynamic adsorption capacity was calculated to be 225.5 mg/g dry resin, very close to the equilibrium capacity of 241.4 mg/g and the resin column could be desorbed by 60 mL of 1% of sodium hydroxide and 75% of ethanol completely.

1. Introduction

p-Hydroxylbenzaldehyde (C_6H_4CHO(*p*-OH)) is a kind of typical aromatic aldehyde and one of the most useful compound in industry. It can be synthesized from phenol by the Reimer–Tiemann or Gattermann reaction and it can also be prepared from *p*-nitrotoluene by a continuous redox, diazotization and hydrolysis reaction. In fact, *p*-hydroxylbenzaldehyde is the primary raw materials for producing a lot of medicines such as amoxicillin, trimethoprimand (TMP), 3,4,5-trimethoxybenzaldehyde and *p*-hydoxygylcine as well as some perfumes such as vanillin, heliotropin and syringaldehyde. However, it is toxic to mankind and it has bad effects on eyes, respiratory system and skins, and hence efficient removal of *p*-hydroxylbenzaldehyde from wastewater is of great importance.

Various porous materials such as zeolites, active carbons, silica gels, metal–organic frameworks (MOFs) and macroporous polymeric adsorbents are very important in many research areas, especially in adsorption, catalysis, energy storage and electrochemistry [1–5]. Among these porous materials, macroporous polymeric adsorbents, especially the newly developed hypercrosslinked poly(styrene-co-divinylbenzene) (PS) resins in 1970s, have been extensively used in various industrial adsorption and separation processes of organic aromatic compounds such as benzene, toluene, β-naphthol and phenol from aqueous solutions [6–8],

* Corresponding author at: College of Chemistry and Chemical Engineering, Central South University, Changsha 410083, China.
E-mail address: jianhanhuang@csu.edu.cn (J. Huang).

1385-8947/$ - see front matter © 2013 Elsevier B.V. All rights reserved.
http://dx.doi.org/10.1016/j.cej.2013.01.020

and they are considered as powerfully potential replacement of activated carbon for organic compounds removal from wastewater. In addition, the hypercrosslinked PS resins have also been widely used for large scale adsorption of organic compounds from gaseous media and for solid-phase extraction of trace components and they are often applied as column packing materials in high-performance liquid chromatography (HPLC) and ion size-exclusion chromatography materials [9–13].

The hypercrosslinked PS resins are usually synthesized from a linear PS or a low cross-linked PS by adding bi-functional/multi-functional cross-linking reagents such as bischloromethylated benzene, trichloromethylatedmesethylene (TCMM), monochlorodimethylether (MCDE) and *p*-dibenzenylchloride and Friedel–Crafts catalysts including anhydrous zinc chloride, iron (III) chloride and stannic (IV) chloride [14]. They can also be prepared from a macroporous low cross-linked chloromethylated PS by two sequential Friedel–Crafts alkylation reaction [15]. After the corresponding reactions, the obtained hypercrosslinked PS networks consist of an intensive bridging of strongly solvated PS chains with conformationally rigid links, leading a major shift of their pore diameter distribution from predominate mesopores to mesopores–micropores bimodal distribution, and hence results in a sharp increase of the Brunauer–Emmet–Teller (BET) surface area and pore volume. Because of these significant changes, the hypercrosslinked PS resin displays very large adsorption capacities towards non-polar and weakly polar aromatic compounds from aqueous solution. In order to increase their adsorption capacities towards polar aromatic compounds, the resins were frequently modified by introducing polar units into the copolymers, using polar compounds as the cross-linking reagent and addition of polar compounds in the Friedel–Crafts reaction [16,17]. The results indicated that the chemically modified hypercrosslinked PS resins exhibited improved adsorption properties towards polar aromatic compounds by introducing certain specific functional groups on their surface.

In this study, we firstly synthesized a type of resorcinol modified hypercrosslinked PS resins, labeled as HJ-H00, HJ-H02, HJ-H05, HJ-H10 and HJ-H15, from macroporous cross-linked chloromethylated PS by adding 0%, 2%, 5%, 10% and 15% of resorcinol in the Friedel–Crafts reaction. After characterizing these resins by nitrogen adsorption–desorption isotherms, chemical analysis, elemental analysis and Fourier transform infrared (FT-IR) spectroscopy, their adsorption selectivity towards benzaldehyde and *p*-hydroxylbenzaldehyde was confirmed by the batch adsorption experiment from aqueous solution. The most promising resin HJ-H02 was thereafter selected for the equilibrium, kinetics and dynamic adsorption of *p*-hydroxylbenzaldehyde from aqueous solution in detail.

2. Experimental method

2.1. Materials and reagents

Macroporous cross-linked chloromethylated PS applied as the synthetic precursor in this study was purchased from Langfang Chemical Co. Ltd. (Hebei, China). Benzaldehyde (Molecular formula: C_6H_5CHO, Molecular weight: 106.1) and *p*-hydroxylbenzaldehyde applied as the adsorbates in the present study were analytical reagents and used without further purification.

2.2. Preparation of resorcinol modified hypercrosslinked PS resins

The preparation procedure for the resorcinol modified hypercrosslinked PS resins was performed according to the Friedel–Crafts reaction in Ref. [8] and the detailed synthetic method was shown in Scheme S1. 1,2-dichloroethane was applied as the solvent and iron (III) chloride was employed as the catalysts in the Friede–Crafts reaction. Additionally, the mass percentage of resorcinol was set to be 0%, 2%, 5%, 10% and 15% relative to the chlorine content of macroporous cross-linked chloromethylated PS (w/w), respectively, and the resorcinol modified hypercrosslinked PS resin named as HJ-H00, HJ-H02, HJ-H05, HJ-H10 and HJ-H15 were synthesized accordingly.

2.3. Equilibrium and kinetic adsorption experiment

Firstly about 0.1000 g of resins was weighed accurately in a series of flasks with a stopper and they were mixed with 50 mL of *p*-hydroxylbenzaldehyde aqueous solution at different initial concentrations. The initial concentrations of *p*-hydroxylbenzaldehyde were set to be 200.1 mg/L, 400.2 mg/L, 600.3 mg/L, 800.4 mg/L and 1000.5 mg/L, respectively. The series of flasks were then shaken in a water-bath thermostatic oscillator (the agitation speed was set to be 200 rpm) for 8 h at a desired temperature (298 K, 308 K or 318 K) so that the adsorption process reach equilibrium (From the kinetic adsorption experiments, it is observed that 8 h is enough for the adsorption reaching equilibrium). After that, the solid resins were filtered and the equilibrium concentration of *p*-hydroxylbenzaldehyde aqueous solution C_e (mg/L) was determined and the equilibrium adsorption capacity q_e (mg/g) was calculated by conducting a mass balance on *p*-hydroxylbenzaldehyde before and after the experiment. The kinetic curves of *p*-hydroxylbenzaldehyde adsorbed on the resin were performed by analyzing the adsorption uptakes on the resin until the equilibrium was reached (the initial concentration of *p*-hydroxylbenzaldehyde was set to be 300.2 mg/L, 500.4 mg/L and 800.1 mg/L, respectively).

2.4. Dynamic adsorption and desorption experiment

2.5740 g of dry resin was accurately weighed and immersed by de-ionized water with the temperature at 298 K for 24 h, then they were packed in a glass column (16 mm diameter) densely to assemble into a resin column and the wet resin column was measured to be 10 mL. 500.4 mg/L of *p*-hydroxylbenzaldehyde aqueous solution was passed through the resin column at a flow rate of 6.0 BV/h (1 BV = 10 mL) and the residual concentration of *p*-hydroxylbenzaldehyde of the effluent *C* (mg/L) was dynamically recorded until it reached the initial concentration. After the dynamic adsorption experiment, the resin column was roughly rinsed by 50 mL of de-ionized water and then a mixed aqueous solution containing 1% of sodium hydroxide and 75% of ethanol was applied as the desorption solvent to the dynamic desorption experiment. The solvent was passed through the resin column at a flow rate of 4.6 BV/h and the concentration of *p*-hydroxylbenzaldehyde from the effluent was determined until it was about zero.

2.5. Analysis

The specific surface area and pore volume of the resin were determined by nitrogen adsorption–desorption isotherms at 77 K using a Micromeritics Tristar 3000 surface area and porosity analyzer. The total specific surface area and pore volume were calculated according to Brunauer–Emmett–Teller (BET) model while the pore size distribution was calculated by applying Barrett–Joyner–Halenda (BJH) method to the nitrogen desorption data. The chorine content of the resin was measured according to a Volhard method in Ref. [18]. The elemental analysis of the resin was performed by a VarioEL Elemental Analysis System and the oxygen content of the resin was calculated as: O (%)=100–C (%)–H (%)–Cl (%). FT-IR spectrum of the resin was collected on a Nicolet 510P Fourier transformed infrared instrument. The weak acid exchange capacity of the resin was performed according to the method in

Ref. [19] using a dilute sodium hydroxide-ethanol solution and the water retention capacity of the resin was determined by the method in Ref. [19]. The concentration of *p*-hydroxylbenzaldehyde in aqueous solution was analyzed via a UV-2450 spectrophotometer at a wavelength of 283.5 nm. To get the residual concentration of *p*-hydroxylbenzaldehyde in aqueous solution, the working curve was firstly determined as: $A = 0.09267C + 0.00687$ with $R^2 = 0.9999$ for the series of standard *p*-hydroxylbenzaldehyde aqueous solutions. The absorbency of the residual *p*-hydroxylbenzaldehyde solution was measured and the residual concentration was calculated based on the working curve.

3. Results and discussion

3.1. Characterization of resorcinol modified hypercrosslinked PS resins

After the reaction, the residual chlorine content sharply decreases from 17.3% (for the chloromethylated PS) to 4.70%, 4.96%, 4.94%, 3.84% and 3.69% for HJ-H00, HJ-H02, HJ-H05, HJ-H10 and HJ-H15, respectively, suggesting that Friedel–Crafts reaction of the chloromethylated PS itself as well as that between the chloromethylated PS and resorcinol may occur in the current reaction system. Particularly, the fact that the absorption intensity of the C–Cl stretching with frequency at 1265 cm^{-1} is greatly weakened after the Friedel–Crafts reaction is a definite evidence for this deduction (see Fig. 1). In addition, Fig. 1 shows that a new moderate vibrational band appears at 1701 cm^{-1} for the resorcinol modified hypercrosslinked resin, this band can be assigned to the stretching of aldehyde carbonyl groups and appearance of this band is due to oxidation of CH_2Cl groups [20,21]. More recently, this band is proven be caused by hindered vibrations of carbon–carbon bonds and valence angles in the aromatic fragments [22]. A wide band related to the stretching of hydroxyl groups at 3425 cm^{-1} is seen in the FT-IR of HJ-H02, HJ-H05, HJ-H10 and HJ-H15 rather than HJ-H00, implying that resorcinol is uploaded on the surface of the resin successfully [23]. The oxygen content of obtained five resins was calculated to be 1.20%, 1.44%, 2.87%, 3.41% and 4.07%, respectively. In particular, the weak acid exchange capacities of the five resins were measured to be 0.008, 0.120, 0.852, 1.104, 1.406 mmol/g, and the water retention capacities of these resins were determined to be 50.6%, 52.8%, 56.6%, 58.5% and 62.7% respectively, which demonstrates that different amounts of aldehyde carbonyl and hydroxyl groups are uploaded on the surface of these resins and these resins show different hydrophilicity.

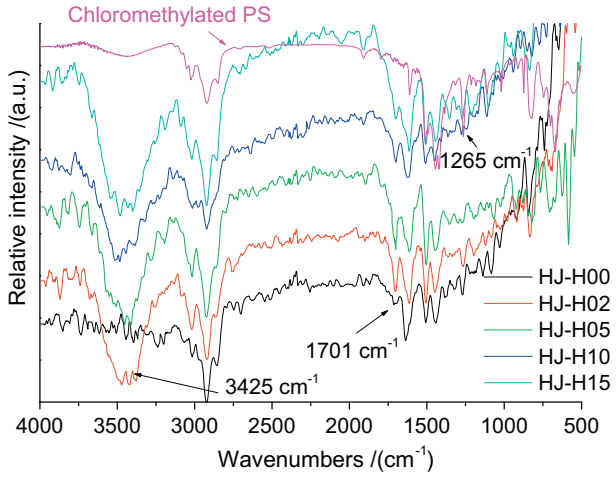

Fig. 1. FT-IR spectra of HJ-H00, HJ-H02, HJ-H05, HJ-H10 and HJ-H15 as well as macroporous cross-linked chloromathylated PS.

All of the nitrogen adsorption–desorption isotherms seem to type-II (see Fig. S1) [24], and mesopores/micropores are the main pores for the modified resins in addition to few macropores even super-macropores (see the pore size distribution in Fig. S2). BET surface area and pore volume of the obtained five resins are sharply increased in comparison with the chloromethylated PS due to the Friedel–Crafts reaction (see Fig. 2). As compared the BET surface area and pore volume of HJ-H02, HJ-H05, HZ-10 and HJ-H15, they decreases with increment of the added mass percentage of resorcinol, which may be resulted from the fact that the Friedel–Crafts reaction between the chloromethylated PS and resorcinol reduces the reaction degree of the chloromethylated PS itself.

3.2. Adsorption selectivity

The five resorcinol modified hypercrosslinked PS resins possesses different chemical structure (different uploading amounts of aldehyde carbonyl and hydroxyl groups on the surface) and pore structure (different BET surface area and pore volume), and hence they should exhibit different adsorption selectivity to different organic compounds. As can be seen from Fig. 3, the equilibrium adsorption capacity of benzaldehyde on HJ-H00 is the largest among the five resins while HJ-H02 has the largest one towards *p*-hydroxylbenzaldehyde. BET surface area and pore volume of HJ-H00 are a little higher than HJ-H02 (1041.7 and 987.8 m^2/g in BET surface area; 0.6813 and 0.6328 cm^3/g in pore volume for HJ-H00 and HJ-H02, respectively), while the surface polarity of HJ-H00 is somewhat less than HJ-H02 (1.20% and 1.44% in oxygen content for HJ-H00 and HJ-H02, respectively). As for the adsorbates, the polarity of *p*-hydroxylbenzaldehyde is much higher than benzaldehyde due to introduction of the hydroxyl group in the *para*-position (the moment dipole of benzaldehyde and *p*-hydroxylbenzaldehyde are measured to be 2.78 D and 4.19 D, respectively [25]). Hence, combinations of the appropriate pore structure and chemical structure of HJ-H02 as well as the excellent matching between *p*-hydroxylbenzaldehyde and HJ-H02 help to bring a better adsorption of *p*-hydroxylbenzaldehyde on HJ-H02 while HJ-H00 has a better adsorption towards benzaldehyde. HJ-H02 is hence employed as a specific polymeric adsorbent for adsorption of *p*-hydroxylbenzaldehyde from aqueous solution in the present study.

3.3. pH effect on the adsorption

Fig. 4 is the equilibrium capacity of *p*-hydroxylbenzaldehyde adsorbed on HJ-H02 as a function of the solution pH. It can be observed that the adsorption is almost steady until the solution

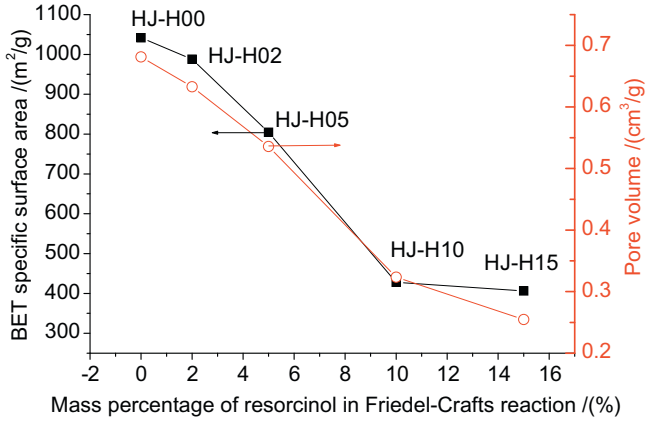

Fig. 2. BET surface area and pore volume of HJ-H00, HJ-H02, HJ-H05, HJ-H10 and HJ-H15.

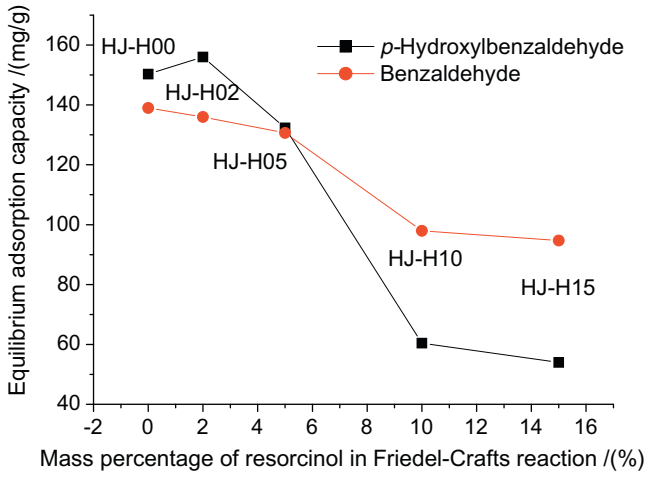

Fig. 3. Comparisons of the equilibrium adsorption capacities of HJ-H00, HJ-H02, HJ-H05, HJ-H10 and HJ-H15 towards *p*-hydroylbenzaldehyde and benzaldehyde from aqueous solution.

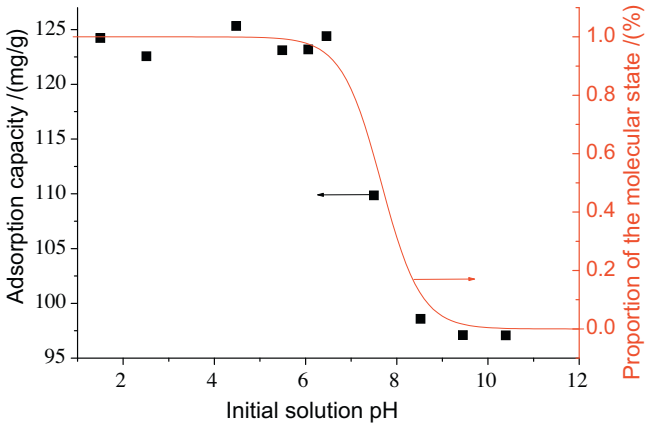

Fig. 4. Equilibrium adsorption capacity of *p*-hydroylbenzaldehyde on HJ-H02 as well as the proportion of the molecular state of *p*-hydroylbenzaldehyde as a function of the solution pH.

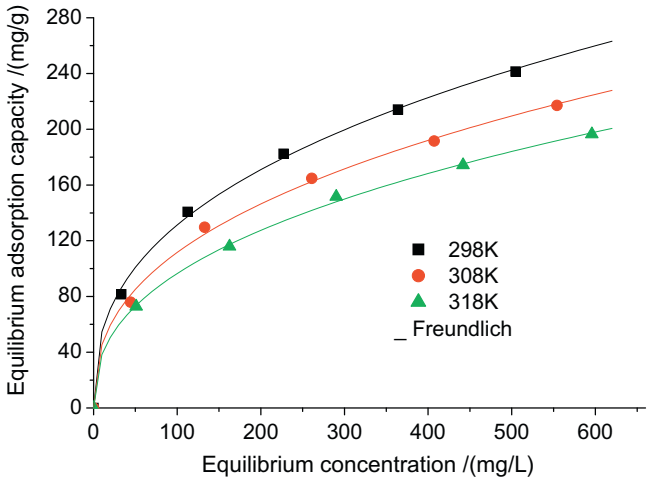

Fig. 5. Equilibrium adsorption isotherms of *p*-hydroylbenzaldehyde on HJ-H02 from aqueous solution with the temperature at 298 K, 308 K and 318 K, respectively.

pH is up to 6.46 and then it decreases rapidly with increasing of the solution pH, the minimum adsorption capacity of *p*-hydroxylbenzaldehyde on HJ-H02 is about 97.0 mg/g. The pK_a of *p*-hydroxylbenzaldehyde is 7.72 and hence the dissociation curve of *p*-hydroxylbenzaldehyde in aqueous solution is also determined and added in Fig. 4. Comparison of the pattern of the adsorption on dependency of the solution pH with the dissociation curve of *p*-hydroxylbenzaldehyde in aqueous solution can reveal that they have the same tendency, suggesting that the molecular form of *p*-hydroxylbenzaldehyde is favorable for the adsorption. In addition, the fact that the minimum adsorption capacity of *p*-hydroxylbenzaldehyde on HJ-H02 is about 97.0 mg/g rather than zero as pH > 8.52 sums up a possible adsorption mechanism of micropore filling due to the micropores of HJ-H02 [26], capillary condensation due to the mesopores of HJ-H02 [24] and π–π stacking due to the benzene ring of HJ-H02 and *p*-hydroxylbenzaldehyde [27] in addition to hydrogen bonding between hydroxyl groups of HJ-H02 and aldehyde carbonyl groups of *p*-hydroxylbenzaldehyde as well as aldehyde carbonyl groups of HJ-H02 and hydroxyl groups of *p*-hydroxylbenzaldehyde [28].

3.4. Adsorption isotherms

Fig. 5 displays the adsorption isotherms of *p*-hydroxylbenzaldehyde on HJ-H02 from aqueous solution. The equilibrium adsorption capacity increases with increasing of the equilibrium concentration and it reaches 241.4 mg/g at an equilibrium concentration of 500.4 mg/L. In addition, a higher temperature results in a weakened adsorption, indicative of an exothermic process [19].

The monolayer Langmuir isotherm can be represented as [29]:

$$q_e = \frac{q_m K_a C_e}{1 + K_a C_e} \quad (1)$$

here q_e is the equilibrium adsorption capacity (mg/g) whereas q_m is the maximum adsorption capacity (mg/g), C_e is the equilibrium concentration of the adsorbate (mg/L) and K_a is the characteristic Langmuir parameter (L/g). The Langmuir equation can be linearized as four different types (see Table 1) and it is proved that a simple linear regression by the four Langmuir equations will result in different results [30].

Additionally, the linear Freundlich equation can be expressed as [31]:

$$\log q_e = \frac{1}{n} \log C_e + \log K_F \quad (2)$$

where K_F ((mg/g)(L/mg)$^{1/n}$) and n are the Freundlich constants.

We have performed a linear fitting by the four linear Langmuir and Freundlich equations and the corresponding parameters are summarized in Table 2, Fig. S3 gives the correlation coefficients R^2. Freundlich equation is obviously more suitable for characterizing the isotherm data due to a higher R^2 (>0.99), suggesting that the present adsorption system is a surface energy heterogeneity.

3.5. Isosteric adsorption enthalpy and surface energy heterogeneity

The isosteric adsorption enthalpy at given fractional loading of the adsorbate (θ, where $\theta = q_e/q_m$) can be calculated by the derivative Clausius–Clapeyron equation as [32]:

$$\log C_e = -\frac{\Delta H}{RT} + C' \quad (3)$$

where ΔH is the isosteric adsorption enthalpy (kJ/mo1), T is the temperature (K) and R is the gas constant (8.314 J/(mol K)). By plotting ln C_e versus $1/T$ at a given fractional loading, the isosteric adsorption enthalpies can be calculated from the slopes. The plots of variation of ΔH for *p*-hydroxylbenzaldehyde adsorption on

Table 1
Four types of linear Langmuir equations.

Type	Linear form	Plot	Parameters
Langmuir-I	$\frac{C_e}{q_e}=\frac{1}{q_m}C_e+\frac{1}{K_a q_m}$	C_e/q_e versus C_e	q_m = 1/slope; K_a = slope/intercept
Langmuir-II	$\frac{1}{q_e}=\left(\frac{1}{K_a q_m}\right)\frac{1}{C_e}+\frac{1}{q_m}$	$1/q_e$ versus $1/C_e$	q_m = 1/intercept; K_a = intercept/slope
Langmuir-III	$q_e=q_m-\left(\frac{1}{K_a}\right)\frac{q_e}{C_e}$	q_e versus q_e/C_e	q_m = intercept; K_a = −1/slope
Langmuir-IV	$\frac{q_e}{C_e}=K_a q_m-K_a q_e$	q_e/C_e versus q_e	q_m = −intercept/slope; K_a = −slope

Table 2
Typical constants for the adsorption of *p*-hydroxylbenzaldehyde on HJ-H02 from aqueous solution according to the four types of Langmuir and Freundlich equations.

T (K)	Langmuir-I		Langmuir-II		Langmuir-III		Langmuir-IV		Freundlich	
	q_m (mg/g)	K_a (L/g)	q_m (mg/g)	K_a (L/g)	q_m (mg/g)	K_a (L/g)	q_m (mg/g)	K_a (L/g)	n	K_F
298	282.5	9.575	245.7	14.74	255.6	13.38	262.5	12.36	2.521	20.84
308	259.1	7.840	232.0	10.83	239.2	10.04	243.8	9.520	2.437	16.56
318	238.1	6.762	204.5	10.59	212.9	9.597	220.9	8.620	2.464	14.79

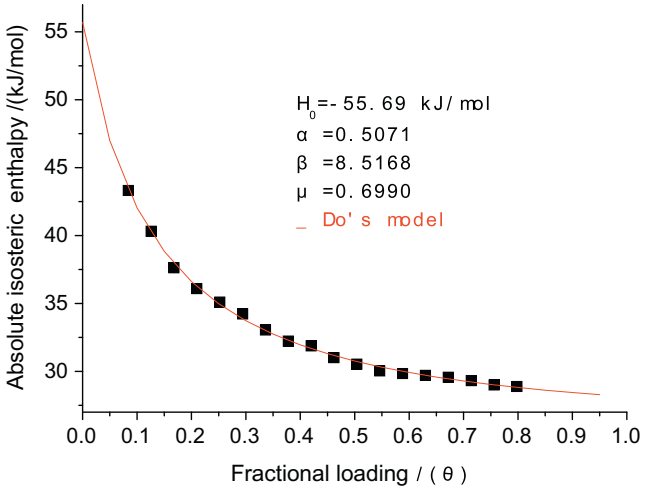

Fig. 6. Isosteric adsorption enthalpies of *p*-hydroylbenzaldehyde on HJ-H02 versus the fraction loading (θ).

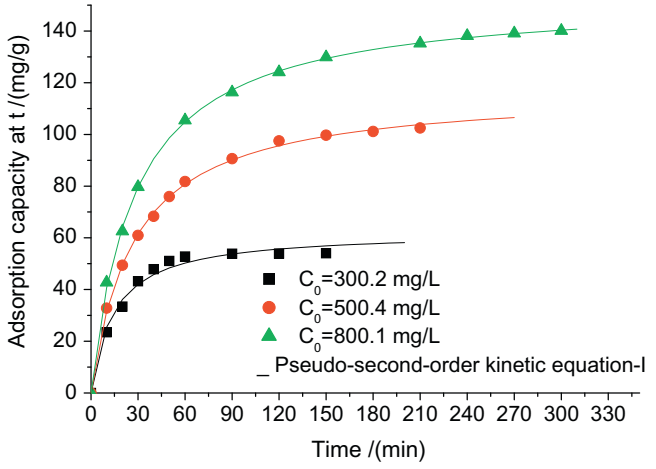

Fig. 7. Kinetic curves of *p*-hydroylbenzaldehyde adsorbed on HJ-H02 from aqueous solution with the initial concentration at 300.2 mg/L, 500.4 mg/L and 800.1 mg/L, respectively.

HJ-H02 are shown in Fig. 6. It is clear that the ΔH decreases with increasing of the fractional loading, indicative of the surface energy heterogeneity. It reaches values typical of physical adsorption (i.e. −20 kJ/mol) at a high fractional loading of about 0.80.

We applied Do's model to account for the surface energy heterogeneity as well as the adsorbate–adsorbate interaction [33]. Do's model takes the isosteric adsorption enthalpy as a function of the fractional loading of the adsorbate as:

$$\Delta H = \Delta H_0\{1-\alpha\beta\theta/[1+(\beta-1)\theta]\}+\mu\theta \quad (4)$$

where ΔH is the isosteric adsorption enthalpy corresponding to the fraction loading, ΔH_0 is the isosteric adsorption enthalpy with $\theta = 0$, α is the variation ratio of the isoteric adsorption enthalpy with θ from 0 to 1 and it reflects the extent of the surface energy heterogeneity of the adsorbent. β is the pattern parameter and a higher β suggests that the fraction of the high-energy adsorption sites of the adsorbent is small. μ is the interaction parameter between the adsorbed adsorbates.

In the present adsorption system, we fit the ΔH against θ to Eq. (4) by a non-linear fitting method and the values of ΔH_0, α, β and μ are obtained and shown in Fig. 4. ΔH_0 is determined to be −55.69 kJ/mol, greater than the energy of physical adsorption and a chemical adsorption is possibly involved for the present system. The value of α is higher than that of the macroporous cross-linked polymeric adsorbents while a little lower than those of some other hypercrosslinked PS resins [27,34,35], indicative of the different adsorption mechanisms between the adsorbents and the adsorbates. The macroporous cross-linked polymeric adsorbents adsorb organic compounds from non-aqueous/aqueous solution mainly through hydrogen bonding [27,34], whereas multiple interactions including hydrogen bonding, micropore filling, capillary condensation and π–π stacking are involved between the hypercrosslinked PS resins and the adsorbates [35]. In addition, the relatively lower value of β of HJ-H02 as well as some other hypercrosslinked PS resins in comparison with the macroporous cross-linked polymeric adsorbents signifies a more fraction of the high-energy sites of the adsorbents.

3.6. Kinetic adsorption

Fig. 7 is the kinetic curves for the adsorption of *p*-hydroxylbenzaldehyde on HJ-H02. It is clear that an increased initial concentration induces a larger equilibrium adsorption capacity while a longer required time from the beginning to the equilibrium (60 min at the initial concentration of 300.2 mg/L while 240 min at 800.1 mg/L), implying that the whole adsorption rate as well as the diffusion rate at a higher initial concentration is lower.

Table 3
Characteristic constants for the kinetic adsorption of *p*-hydroxylbenzaldehyde on HJ-H02 from aqueous solution according to the pseudo-first-order and four types of linear pseudo-second-order kinetic equations.

Kinetic equation type	Parameters	C_0 = 300.2 mg/L	C_0 = 500.4 mg/L	C_0 = 800.1 mg/L
Pseudo-first-order rate equation	q_e (mg/g)	65.07	88.71	113.8
	k_1 (1/min)	2.774×10^{-2}	1.015×10^{-2}	7.250×10^{-3}
	R^2	0.9936	0.9976	0.9890
Pseudo-second-order rate equation-I	q_e (mg/g)	59.38	116.2	153.4
	k_2 (g/(mg min))	1.466×10^{-3}	3.287×10^{-4}	2.361×10^{-4}
	R^2	0.9956	0.9996	1.000
Pseudo-second-order rate equation-II	q_e (mg/g)	65.57	114.7	150.2
	k_2 (g/(mg min))	8.586×10^{-4}	3.439×10^{-4}	2.588×10^{-4}
	R^2	0.9826	0.9980	0.9968
Pseudo-second-order rate equation-III	q_e (mg/g)	63.81	116.3	152.2
	k_2 (g/(mg min))	9.728×10^{-4}	3.268×10^{-4}	2.456×10^{-4}
	R^2	0.9113	0.9934	0.9942
Pseudo-second-order rate equation-IV	q_e (mg/g)	65.55	116.6	152.3
	k_2 (g/(mg min))	8.627×10^{-4}	3.238×10^{-4}	2.441×10^{-4}
	R^2	0.9113	0.9934	0.9942

Lagergren's first-order rate equation is the earliest known one describing the adsorption rate, and its linear equation can be followed as [36]:

$$\log(q_e - q_t) = \log q_e - k_1 t \tag{5}$$

here k_1 is the pseudo-first-order rate constant (min^{-1}) and q_t (mg/g) is the adsorption capacity at the contact time t.

On the other hand, pseudo-second-order equation proposed by Ho and McKay can be expressed as [37,38]:

$$\frac{dq}{dt} = k_2(q_e - q_t)^2 \tag{6}$$

where k_2 is the pseudo-second-order rate constant (g/(mg min)). If integration of Eq. (7), the pseudo-second-order kinetic model can be linearized as four different types (see Table S1).

The kinetic data in Fig. 7 are fitted by the Lagergren's first-order and pseudo-second-order rate equations, k_1, k_2, q_e and R^2 are listed in Table 3. It can be found that the pseudo-second-order kinetic equation-I is the most suitable. In addition, the calculated k_2 increases with increasing of the initial concentration, accordant with the observed phenomena above.

3.7. Dynamic adsorption and desorption

As can be seen from Fig. 8a, the breakthrough point (C/C_0 = 0.05) for *p*-hydroxylbenzaldehyde adsorption on HJ-H02 is 59.8 BV. The dynamic adsorption capacity can be calculated to 58.04 mg/mL wet resin (or 225.5 mg/g dry resin) by using a numerical integration method. This value is very close to the equilibrium adsorption capacity of 241.4 mg/g, revealing that the consistency between the equilibrium and the dynamics, it also confirms that HJ-H02 is really an efficient polymeric adsorbent for adsorption of *p*-hydroxylbenzaldehyde from aqueous solution.

Thomas and Clark models are two typical dynamic models for the dynamic adsorption [39]. Thomas model can be expressed as:

$$\frac{C}{C_0} = \frac{1}{1 + \exp[k_T(q_0 m_C - C_0 V_{eff})/Q]} \tag{7}$$

where C is the concentration of the adsorbate from the effluent, C_0 is the initial concentration of the adsorbate, k_T is the Thomas rate constant (L/(min mg)), q_0 is the maximum adsorption capacity of the adsorbate on the adsorbent (mg/g), m_C is the weight of the adsorbent in the column (g), V_{eff} is the throughput volume (L) and Q is the volumetric flow rate (L/min).

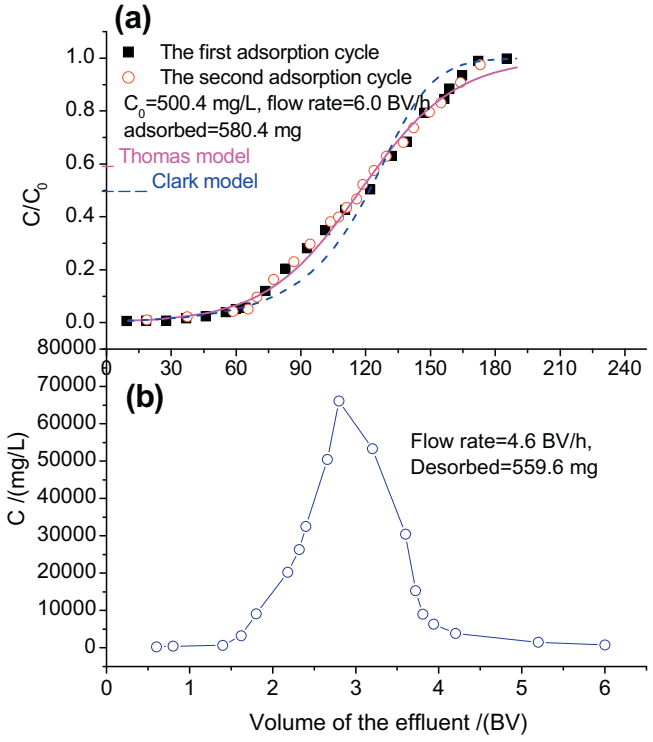

Fig. 8. Dynamic adsorption (a) and desorption (b) curves of *p*-hydroylbenzaldehyde on HJ-H02 from aqueous solution.

Clark applied the mass-transfer coefficient in combination with the Freundlich equation to define a new relation as [40]:

$$\frac{C}{C_0} = \left(\frac{1}{1 + Ae^{-rt}}\right)^{1/n-1} \tag{8}$$

where n is the Freundlich constant, A and r are the constants related to the breakthrough point.

The dynamic data in Fig. 8a are fitted by Thomas and Clark models using a non-linear regression. It can be observed that the Thomas model fits the dynamic curve better than the Clark model. The corresponding calculated parameter of $k_T = 5.499 \times 10^{-4}$ (L/(min mg)) is close to the fitted result by the pseudo-second-order rate equation-I (3.287×10^{-4}).

After the dynamic adsorption experiment, the resin column is subjected to a mixed aqueous solution containing 1% of sodium hydroxide and 75% of ethanol, and it is seen that 60 mL of the solution can desorb the resin column completely (see Fig. 8b). The dynamic desorption capacity from the resin column is calculated to be 559.6 mg, which is very close to the dynamic adsorption capacity (580.4 mg). We also perform a second dynamic adsorption experiment after regeneration of the resin column. It is shown in Fig. 8a that the second dynamic curve is almost identical to the first one, which further indicates that the resin column can be regenerated completely and it can be used repeatedly.

4. Conclusions

In the present study, we have synthesized a series of resorcinol modified hypercrosslinked PS resins, HJ-H00, HJ-H02, HJ-H05, HJ-H10 and HJ-H15, and they were tested for adsorption of *p*-hydroxylbenzaldehyde from aqueous solution. The oxygen content of five resins was calculated to be 1.20%, 1.44%, 2.87%, 3.41% and 4.07%, and their BET surface area were measured to be 1041.7, 987.8, 804.5, 428.0 and 406.5 m^2/g, respectively, which is indicative of their different chemical structure and pore structure.

The molecular state of *p*-hydroxylbenzaldehyde was suitable for the adsorption and the mechanism was based on hydrogen bonding, micropore filling, capillary condensation and π–π stacking. Freundlich equation was suitable for the equilibrium data. The isosteric adsorption enthalpies decreased with increasing of the fractional loading, suggesting that HJ-H02 was an adsorbent with surface energy heterogeneity and surface energy heterogeneity could be characterized by Do's model successfully. The pseudo-second-order rate equation-I was appropriate for the kinetic data. The dynamic adsorption capacity of *p*-hydroxylbenzaldehyde on HJ-H02 was measured to be 58.04 mg/mL wet resin and Thomas model was suitable for the dynamic adsorption, the resin column could be regenerated completely and the resin could be used repeatedly.

Acknowledgments

The National Natural Science Foundation of China (No. 21174163) and the Shenghua Yuying Project of Central South University are gratefully appreciated for the financial supports.

Appendix A. Supplementary material

Supplementary data associated with this article can be found, in the online version, at http://dx.doi.org/10.1016/j.cej.2013.01.020.

References

[1] N. Fontanals, R.M. Marcé, F. Borrull, New materials in sorptive extraction techniques for polar compounds, J. Chromatogr. A 1152 (2007) 14–31.
[2] M. Hartmann, A. Vinu, G. Chandrasekar, Adsorption of vitamin E on mesoporous carbon molecular sieves, Chem. Mater. 17 (2005) 829–833.
[3] Y. Wang, P.T.M. Nguyen, N. Sakao, T. Horikawa, D.D. Do, K. Morishige, D. Nicholson, Characterization of a new solid having graphitic hexagonal pores with a GCMC technique, J. Phys. Chem. C 115 (2011) 13361–13372.
[4] J.L.C. Rowsell, O.M. Yaghi, Metal–organic frameworks: a new class of porous materials, Micropor. Mesopor. Mater. 73 (2004) 3–14.
[5] M.P. Tsyurupa, V.A. Davankov, Hypercrosslinked polymers: basic principle of preparing the new class of polymeric materials, React. Funct. Polym. 53 (2002) 193–203.
[6] A.M. Li, Q.X. Zhang, G.C. Zhang, J.L. Chen, Z.H. Fei, F.Q. Liu, Adsorption of phenolic compounds from aqueous solutions by a water-compatible hypercrosslinked polymeric adsorbent, Chemosphere 47 (2002) 981–989.
[7] B.C. Pan, W.M. Zhang, B.J. Pan, H. Qiu, Q.R. Zhang, Q.X. Zhang, S.R. Zheng, Efficient removal of aromatic sulfonates from wasterwater by a recyclable polymer: 2-naphthalene sulfonate as a representative pollutant, Environ. Sci. Technol. 42 (2008) 7411–7416.
[8] J.H. Ahn, J.E. Jang, C.G. Oh, S.K. Ihm, J. Cortez, D.C. Sherrington, Rapid generation and control of microporosity, bimodal pore size distribution, and surface area in davankov-type hyper-cross-linked resins, Macromolecules 39 (2006) 627–632.
[9] V. Davankov, M. Tsyurupa, M. Ilyin, L. Pavlova, Hypercross-linked polystyrene and its potentials for liquid chromatography: a mini-review, J. Chromatogr. A 965 (2002) 65–73.
[10] D. Bratkowska, R.M. Marcé, P.A.G. Cormack, D.C. Sherrington, F. Borrull, N. Fontanals, Synthesis and application of hypercrosslinked polymers with weak cation-exchange character for the selective extraction of basic pharmaceuticals from complex environmental water samples, J. Chromatogr. A 1217 (2010) 1575–1582.
[11] M. Laatikainen, T. Sainio, V. Davankov, M. Tsyurupa, Z. Blinnikova, E. Paatero, Chromatographic separation of a concentrated HCl–$CaCl_2$ solution on non-ionic hypercrosslinked polystyrene, React. Funct. Polym. 67 (2007) 1589–1598.
[12] C. Long, Y. Li, W.H. Yu, A.M. Li, Adsorption characteristics of water vapor on the hypercrosslinked polymeric adsorbent, Chem. Eng. J. 180 (2012) 106–112.
[13] D. Bratkowska, N. Fontanals, F. Borrull, P.A.G. Cormack, D.C. Sherrington, R.M. Marcé, Hydrophilic hypercrosslinked polymeric sorbents for the solid-phase extraction of polar contaminants from water, J. Chromatogr. A 1217 (2010) 3238–3243.
[14] M.P. Tsyurupa, V.A. Davankov, Porous structure of hypercrosslinked polystyrene: state-of-the-art mini-review, React. Funct. Polym. 66 (2006) 768–779.
[15] J.H. Huang, K.L. Huang, S.Q. Liu, A.T. Wang, C. Yan, Adsorption of Rhodamine B and methyl orange on a hypercrosslinked polymeric adsorbent in aqueous solution, Colloids Surf. A 330 (2008) 55–61.
[16] V.V. Azanova, J. Hradil, Sorption properties of macroporous and hypercrosslinked copolymers, React. Funct. Polym. 41 (1999) 163–175.
[17] J. Hradil, E. Králová, Styrene-divinylbenzene copolymers post-crosslinked with tetrachloromethane, Polymer 39 (1998) 6041–6048.
[18] C.P. Wu, C.H. Zhou, F.X. Li, Experiments of Polymeric Chemistry, Anhui Science and Technology Press, Hefei, 1987.
[19] B.L. He, W.Q. Huang, Ion Exchange and Adsorption Resin, Shanghai Science and Technology Education Press, Shanghai, 1995.
[20] M.C. Xu, Z.Q. Shi, B.L. He, Structure and properties of hypercrossliked polymeric adsorbents, Acta Polym. Sin. 4 (1996) 446–449.
[21] G.H. Meng, A.M. Li, W.B. Yang, F.Q. Liu, X. Yang, Q.X. Zhang, Mechanism of oxidative reaction in the postcrosslinking of hypercrosslinked polymers, Eur. Polym. J. 43 (2007) 2732–2737.
[22] M.P. Tsyurupa, Z.K. Blinnikova, Y.A. Davidovich, S.E. Lyubimov, A.V. Naumkin, V.A. Davankov, On the nature of "functional groups" in non-functionalized hypercrosslinked polystyrenes, React. Funct. Polym. 72 (2012) 973–982.
[23] J.T. Wang, Q.M. Hu, B.S. Zhang, Y.M. Wang, Organic Chemistry, Nankai University Press, Tianjing, 1998.
[24] D.D. Do, Adsorption Analysis: Equilibria and Kinetics, World Scientific Publishing, Singapore, 1998.
[25] I.M. El-Anwar, I.Z. Selim, Dielectric properties of some aldehydes, J. Mater. Sci. Technol. 11 (1995) 222–228.
[26] D.M. Ruthve Duong, Principles and Adsorption and Adsorption Processes, Willey Inter-science, New York, 1984.
[27] H.T. Li, M.C. Xu, Z.Q. Shi, B.L. He, Isotherm analysis of phenol adsorption on polymeric adsorbents from nonaqueous solution, J. Colloid Interface Sci. 271 (2004) 47–54.
[28] J.H. Huang, K.L. Huang, S.Q. Liu, Q. Luo, M.C. Xu, Adsorption properties of tea polyphenols onto three polymeric adsorbents, with amide group, J. Colloid Interface Sci. 315 (2007) 407–414.
[29] I. Langmuir, The constitution and fundamental properties of solids and liquids, J. Am. Chem. Soc. 38 (1916) 2221–2295.
[30] Y.S. Ho, G. McKay, Sorption of dye from aqueous solution by peat, Chem. Eng. J. 70 (1998) 115–124.
[31] H.M.F. Freundlich, Uber die adsorption in losungen, Z. Phys. Chem. 57A (1906) 385–470.
[32] H.T. Li, Y.C. Jiao, M.C. Xu, Z.Q. Shi, B.L. He, Thermodynamics aspect of tannin sorption on polymeric adsorbents, Polymer 45 (2004) 181–188.
[33] D.D. Do, H.D. Do, A new adsorption isotherm for heterogeneous adsorbent based on the isosteric heat as a function of loading, Chem. Eng. Sci. 52 (1997) 297–310.
[34] J.H. Huang, Y. Zhou, K.L. Huang, S.Q. Liu, Q. Luo, M.C. Xu, Adsorption behavior, thermodynamics, and mechanism of phenol on polymeric adsorbents with amide group in cyclohexane, J. Colloid Interface Sci. 316 (2007) 10–18.
[35] W.M. Zhang, Z.W. Xu, B.C. Pan, C.H. Hong, K. Jia, P.J. Jiang, Q.J. Zhang, B.J. Pan, Equilibrium and heat of adsorption of diethyl phthalate on heterogeneous adsorbents, J. Colloid Interface Sci. 325 (2008) 41–47.
[36] S. Lagergren, About the theory of so-called adsorption of soluble substances, Kungliga Svenska Vetenskapsakademiens, Handlingar, Band 24 (1898) 1–39.
[37] Y.S. Ho, G. McKay, Pseudo-second order model for sorption processes, Process Biochem. 34 (1999) 451–465.
[38] Y.S. Ho, Review of second-order models for adsorption systems, J. Hazard. Mater. 136 (2006) 681–689.
[39] H.C. Thomas, Heterogeneous ion exchange in a flowing system, J. Am. Chem. Soc. 66 (1944) 1664–1666.
[40] R.M. Clark, Evaluating the cost and performance of field-scale granular activated carbon systems, Environ. Sci. Technol. 21 (1987) 573–580.